## Contribution of Unbroken Strands to the Fracture of

## Polymer Networks

Shu Wang, † Sergey Panyukov, \*\* ‡, \$ Stephen Craig, \*\* † Michael Rubinstein \*\* †, §, #

<sup>†</sup>Department of Chemistry, Duke University, Durham, NC 27708-0346, United States

<sup>‡</sup>P. N. Lebedev Physics Institute, Russian Academy of Sciences, Moscow 117924, Russia

<sup>\$</sup>Department of Theoretical Physics, Moscow Institute of Physics and Technology, 141700, Russia

§Department of Mechanical Engineering and Materials Science, Biomedical Engineering, and

Physics, Duke University, Durham, NC 27708-0300, United States

\*Institute for Chemical Reaction Design and Discovery (WPI-ICReDD), Hokkaido University,

Sapporo 001-0021, Japan

ABSTRACT. We present a modified Lake-Thomas theory that accounts for the molecular details of network connectivity upon crack propagation in polymer networks. This theory includes not only the energy stored in the breaking network strands (bridging strands) but also the energy stored in the tree-like structure of the strands connecting the bridging strands to the network continuum, which remains intact as the crack propagates. The energy stored in each of the generations of this tree depends non-monotonically on the generation index due to the nonlinear elasticity of the stretched network strands. Further, the energy required to break a single bridging strand is not necessarily dominated by the energy stored in the bridging strand itself, but in the higher generations of the tree. We describe the effect of mechanophores with stored length on the energy

stored in the tree-like structure. In comparison with the "strong" mechanophores that can only be activated in the bridging strand, "weak" mechanophores that can be activated both in the bridging strand and in other generations could provide more energy dissipation due to their larger contribution to higher generations of the tree.

Introduction. The lifetime and the utility of polymer networks are often restricted by their fracture, which involves the mechanical scission of covalent polymer strands within the network. The fracture of networks is typically discussed in terms of its tearing energy, which quantifies the resistance of a network to crack propagation. 1-3 The tearing energy has a critical value, which is defined by the minimum energy required to create a unit of the new surface. 1,2,4 Due to the lack of direct characterization of molecular behaviors at the crack tip, the energy required to break each bridging strand in the network that enters the critical tearing energy of the network remains unclear.<sup>5–7</sup> Hence, a quantitative molecular model that can provide physical and chemical insight into the molecular behaviors at the crack tip is needed for a detailed description of the fracture of polymer networks. The critical tearing energy of polymer networks has been extensively studied using the approach of fracture mechanics, in which the network is usually considered as an elastic continuum.<sup>3</sup> On small length scales, however, the network cannot be described as a continuous elastic body since it consists of tree-like structures of polymer chains that are "liquid-like"; the relevant length scale of this transition from continuum to molecular behavior is given by the topological loop size. <sup>8,9</sup> Current molecular models that estimate the network critical tearing energy mainly take into account only the energy of ruptured polymer strands (strands that originally bridge the crack interface) under crack propagation, 1,5,6 but they often ignore the role of the remainder of the tree-like structure<sup>10</sup> within the characteristic topological loop<sup>8,9</sup>. In the next few paragraphs, we first introduce both the macroscopic viewpoint<sup>2</sup> that has been well established in fracture

mechanics and review the molecular models that have been developed to estimate the critical tearing energy. We then present a new model that takes into account the contributions of the tree-like structure of a network in the context of topological loop analysis to connect the molecular and the macroscopic length scales.

Consider a thin elastic network infinite in the horizontal direction with a semi-infinite crack (**Figure 1a**). The sample under vertical load can be divided into three zones: two zones that are further from the crack than the sample height (shaded in light and dark grey in **Figure 1b**), and the zone in the vicinity of the crack (shaded in red in **Figure 1b**). The light grey zone on the left is already relaxed and does not experience any significant stress, while the dark grey zone on the right is almost uniformly deformed and does not yet "feel" the crack. As the crack propagates, the energy released from the sample per newly created surface defines the tearing energy  $\Gamma$ .

Assuming that energy is not dissipated during the elastic deformation of the material, the energy released is the elastic energy that was originally stored in the material during crack propagation. Consider a slice in the dark grey zone that is uniformly deformed. The stress-stretch curve of the material is shown in **Figure 1c**. When the crack propagates, the stretch in the dark grey zone is  $\lambda = \lambda_c$ . The elastic energy stored per unit volume in this part of the sample is the shaded area under the stress-stretch curve  $\int_1^{\lambda_c} \sigma \, d\lambda$ . During the crack propagation, the red region shifts in an invariant way: the dimensions, volume, and distribution of stresses relative to the position of the crack remain unchanged. The energy dissipated by the crack is the energy decrease of the dark grey zone on the right in **Figure 1d** due to the decrease in the volume of this zone. The elastic energy released when a new surface with area  $\Delta A$  is created can be written as  $H\Delta A \int_1^{\lambda_c} \sigma \, d\lambda$ . Hence, the tearing energy is  $\Gamma = H \int_1^{\lambda_c} \sigma \, d\lambda$ . Under the conditions of the slow displacement of the crack and

assuming no hysteresis in the bulk material, elastic energy stored in the material is only released in a small process zone ( $r_p \ll H$ , see **Figure. 1d**) near the crack tip,<sup>11</sup> where the elastic energy is irreversibly dissipated through the damage of the material. Since the tearing energy  $\Gamma$  is a material's property, the critical stretch  $\lambda_c$  at which crack propagates varies with sample height H in such a way that  $\Gamma = H \int_1^{\lambda_c} \sigma \, d\lambda$  does not depend on sample height H.

When it comes to the covalent polymer network with low hysteresis in the bulk, the energy stored in the network can only be dissipated (transferred into heat) through the relaxation of polymer strands, which is triggered by the scission of chemical bonds. The dissipated energy at the process zone in such polymer networks is the critical tearing energy. Therefore, current ideas on the molecular nature of the network critical tearing energy are mainly focused on understanding the rupture of network strands at the crack tip.

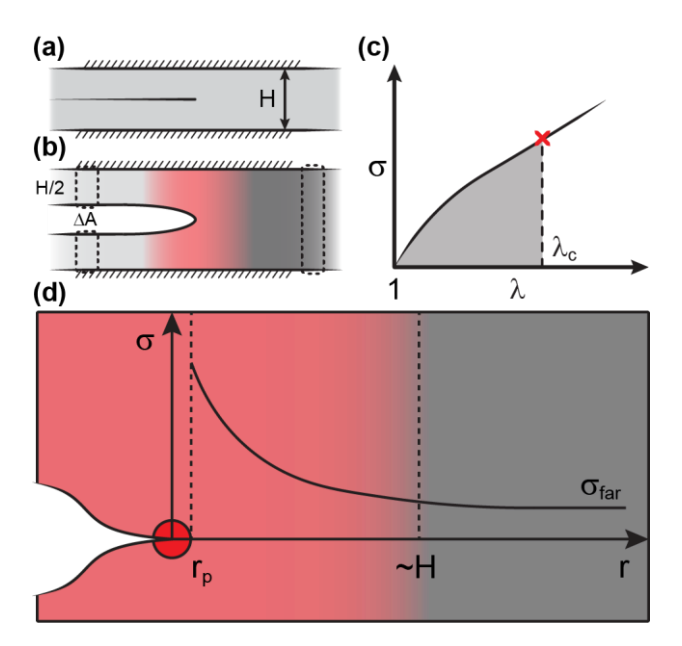


**Figure 1.** (a) A network plate infinite in the horizontal direction with a semi-infinite crack is (b) loaded vertically. The sample can be divided into three zones, two far zones that are far away from

the crack (light grey on the left and dark grey on the right indicate uniformly undeformed and deformed, respectively) and the near zone around the crack (red). (c) Engineering stress-stretch curve of the material. (d) Stress field of the near zone and the far zone. Process zone  $r_p$  is highlighted with the bright red circle.

From the molecular perspective, the fracture of the network is caused by the rupture of elastically active chains that originally bridge the crack interface (bridging strands). 1,12,13 The rupture of bridging strands defines a minimum, intrinsic tearing energy because the potential energy that is released by the relaxation of the breaking strand is not redistributed to the other strands, but is completely dissipated as heat and thus contributes to  $\Gamma$ . According to Lake and Thomas, the critical tearing energy  $\Gamma$  (without contribution from bulk dissipation) per unit area of undeformed new surface created by the crack (see **Figure 1b**) is equal to the number of elastically active bridging strands per cross-sectional area ( $\beta \approx vR_0$ ) (**Figure 2** inset a), multiplied by the critical energy required to break each bridging strand ( $\widehat{U}_{break}$ ) (**Figure 2** inset b):

$$\Gamma = \beta \widehat{U}_{break} \approx v R_0 U_0(f_{break}) \tag{1}$$

where v is the number density of elastically active strands,  $R_0$  is the average end-to-end distance of an elastically active strand in the undeformed network, and  $U_0(f_{break})$  is the energy stored in the bridging strand at the time of fracture.

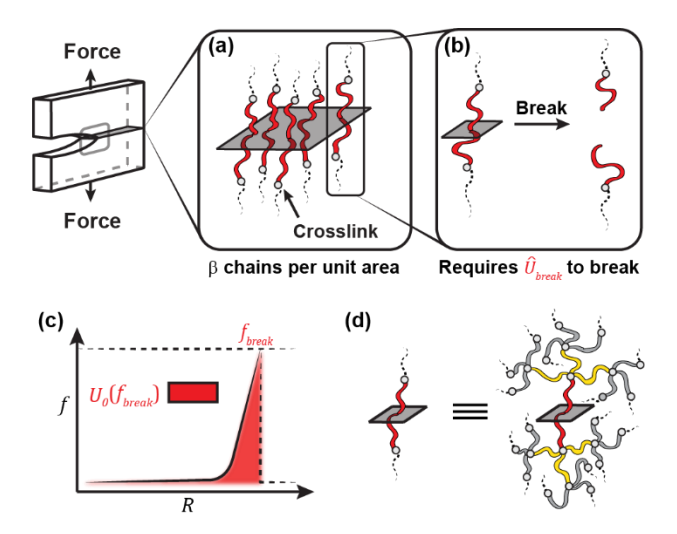


Figure 2. The Lake-Thomas theory predicts that the critical tearing energy  $\Gamma_0$  is equal to the product of (a) the areal number density of bridging strands  $\beta$  and (b) the energy required to break one such bridging strand  $\widehat{U}_{break}$ . The original Lake-Thomas theory only takes into account the energy stored in the bridging strand when it breaks  $\widehat{U}_{break} = U_0(f_{break})$ , which is (c) the area under the force-extension curve of the bridging strand up to the breaking extension. To break the bridging strand, other (unbroken) strands connected to the bridging strand deform and store elastic energy, that dissipates when the bridging strand breaks and this energy must also be taken into consideration. The energy  $\widehat{U}_{break}$  stored at the moment of scission of the bridging strand is essentially elastic energy stored in (d) the tree-like structure. The continuum deforms elastically, and the energy stored in it is dissipated through the scission of tree-like structures. Different colors indicate different generations of the tree.

The extension of bridging strands is accompanied by the extension of other (unbroken) network strands (**Figure 2d**) that are connected to the bridging strands. Based on this concept, Lin and Zhao examined the energy put into multiple generations of a Cayley tree structure with the root at the bridging strand.<sup>10</sup> Once a bridging strand is broken, unbroken strands of this tree are partially

relaxed, and the corresponding part of the elastic energy stored in those strands is dissipated rather than transferred within the invariant process zone. Lin and Zhao assumed that the main contribution to the energy stored in each chain is made by the enthalpy of its linear stretching. In this case, the energy released in each generation of the Cayley tree decays exponentially with distance along the tree from the bridging strand (**Figure 3a**). Since the tree is symmetric, it has two branches rooted in the bridging strand. The positive and negative generations simply represent two directions relative to the bridging strand. Compared to the original Lake-Thomas theory, the Lin-Zhao model modified the energy term  $\hat{U}_{break}$  by an additional numerical factor of z/(z-2), where z is the functionality of the network.

In this paper, we propose a network fracture model which predicts a non-monotonic dependence on energy  $U_g$  stored per generation on the generation index g (the number of network strands along the tree from the bridging strand) (Figure 3b). We show that depending on the network structure, the main contribution to the energy stored in the tree of network strands does not necessarily come from the bridging strand. We apply this analysis in the context of the topological loop size, which describes the crossover between elastic energy that is transferred within the propagating, invariant process zone and elastic energy that is dissipated as heat within a local, liquid-like region (Figure 3c). For a network with monodisperse strands between crosslinks and without defects and entanglements, the size of this crossover topological loop (circle in Figure 3c) is on the order of the size of the process zone mentioned above (red circle in Figure 1d) because the energy originally stored in the continuum is assumed to be released exclusively in the process of relaxation of tree structures (in an elastically deforming continuum, this energy is redistributed between neighboring chains; we treat the case where viscous dissipation in this region is assumed to be negligible and can be ignored). On length scales smaller than the loop size (in the red shaded

process zone in **Figure 3c**; the loops are highlighted in red), trees rooted from different bridging strands are assumed to be independent, as they have not yet "realized" that they are in the same loops with other trees. On scales larger than the loop size, the network can be described by continuum mechanics.

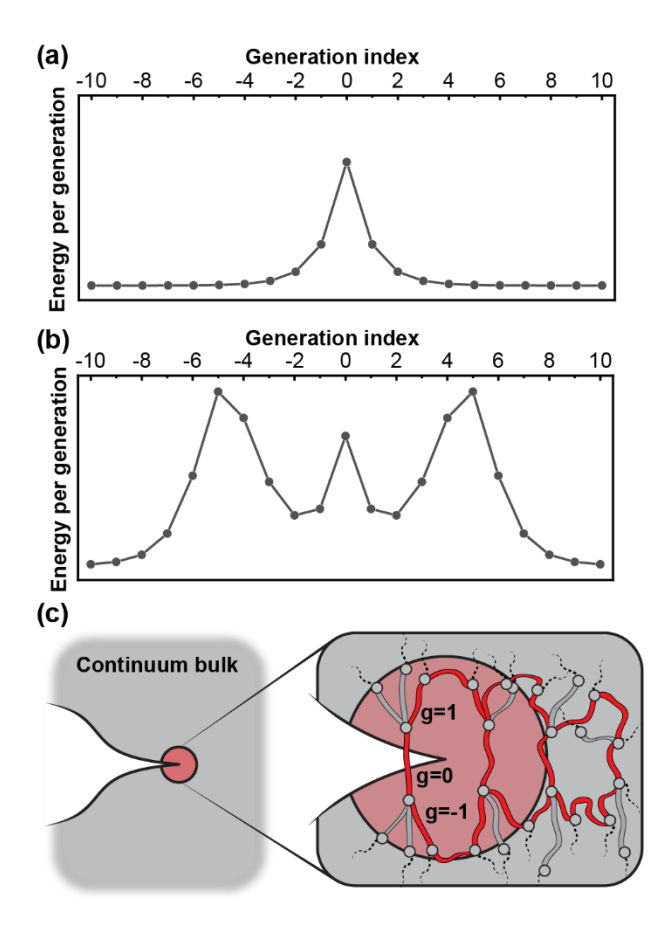


**Figure 3.** (a) Monotonic dependence of energy stored in the tree generations on the absolute value of generation index predicted by Lin and Zhao (ref). (b) Non-monotonic dependence of energy predicted by the current model (eq. 3, 8). (c) The length scale of the crossover between tree structures and the continuum bulk at the crack tip is determined by the average topological loop

size in the polymer networks. The topological loops formed by interconnected trees of different bridging strands are highlighted by red color.

As we show below, the non-monotonic dependence of energy  $U_g$  stored in the generation of the tree structure with generation index g originates from the non-linear entropic elasticity of polymer chains. To understand the origin of such non-monotonic dependence, we analyze the condition that gives the extremes of the energy per generation. The distribution of the energy per generation along the tree structure is discussed for various parameters (functionality, breaking tension, entropic elasticity, and energetic elasticity of chain segments). Using the concept of a tree structure, we further discuss how to design mechanophores to achieve larger critical tearing energy in polymer networks.

Elastic energy stored in a "tree-like" structure ( $\hat{U}$ ). Imagine a defect-free unentangled polymer network that is formed by an end-linking solution or melt of monodisperse polymer chains. In such networks, tree structures have at least several generations.<sup>8,9,14</sup> As the crack propagates, tension is focused onto some strands, that become the bridging strands. Therefore, the bridging strands have higher tension than other strands which do not bridge the crack surface. For each bridging strand, we can imagine a tree structure shown in **Figure 2d**. We ignore both viscous energy dissipation and chain scission in the continuum by assuming a relatively low deformation rate and small loss modulus G" at this rate and chain tension in the continuum being much lower than critical. Therefore, during the crack propagation, the energy stored in the continuum is redistributed between its chains, transferred to the tree-like structure at the crack surface, and released there through the scission of bridging strands, since in this case, the chain scission in the process zone

is the only mechanism for energy dissipation. Once a bridging strand is broken, most of the elastic energy stored in that tree-like structure is released, and a loop is opened (**Figure 3c**). The scission of the bridging strand determines the energy stored in a tree structure, and as established in polymer mechanochemistry, the scission of the bridging strand is controlled by the tension applied to it.  $^{12,15,16}$  Hence, it is useful to express the energy stored in a tree  $\hat{U}$  as a function of the tension in the bridging strand  $f_0$ .

The energy stored in the network strand upon its loading is given by the general expression in terms of the force f (**Figure 2c**):

$$U(f) = \int_0^R f' dR = fR(f) - \int_0^f R(f') df'$$
 (2)

As the strands near the crack tip are highly extended, we assume that the strands in the same generation g are parallel to each other, and that they share similar displacement  $R(f_g)$  and force  $f_g$  (Figure 4). According to the force balance condition, the sum of all tensions in each generation is the same, and it is equal to the tension in the bridging strand  $f_0$ . Thus, the tension in a strand of the generation g, is given by  $f_g = f_0/(z-1)^{|g|}$ , where z is the crosslink functionality. The energy stored in a network strand located in the generation g is given by  $U(f_g) = U(f_0/(z-1)^{|g|})$ . The combined energy stored in all  $(z-1)^{|g|}$  chains of generation g is

$$U_g = (z-1)^{|g|} U(f_g) = (z-1)^{|g|} U\left(\frac{f_0}{(z-1)^{|g|}}\right)$$
(3)

Therefore, the total energy  $\widehat{U}$  stored in a tree can thus be written as the sum of  $U_g$ :

$$\widehat{U}(f_0) = \sum_g U_g = \sum_g (z - 1)^{|g|} U\left(\frac{f_0}{(z - 1)^{|g|}}\right)$$
(4)

The dependence of  $\widehat{U}$  on  $f_0$  raises a critical issue: in order for strand scission to occur on any timescale that is relevant to real crack propagation, the required bridging strand tension is kinetically determined. Thus, the specific value of  $f_0$  that is relevant to a given network fracture problem will depend both on the chemical composition of the strand (mechanism of the scission reaction) and on the loading rate of bridging strands at the propagating crack front. The force dependence of mechanochemical reactions has been examined in detail previously,  $^{16}$  and so an appropriate value of  $f_0$  can be chosen based on the system and mechanical conditions under investigation. We note that, in practice, the scission of conventional polymer strands tends to involve tensions on the order of 3-5 nN. Because the force changes by 0.1 nN per decade of variation in timescale, the error introduced by uncertainty in the precise loading-rate dependent value of  $f_0$  is typically expected to be quite small.

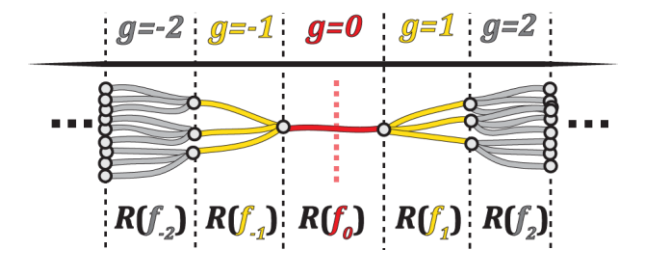


**Figure 4.** A schematic illustration of a tree structure with crosslink functionality z=4 at the crack tip. Different colors indicate the generation index of strands (red < yellow < gray). All strands have the same dependence of extension on applied force R(f) but they have different tensions  $f_g$  depending on their generation. The red dash line indicates the crack path.

Energy profile of a tree-like structure. The Lake-Thomas theory considers the energy stored only in bridging strands, while the Lin-Zhao model considers the energy stored in a tree-like structure, which is equal to the prediction of the Lake-Thomas theory multiplied by a pre-factor related to the functionality of the networks. This Lin-Zhao prediction is the consequence of their assumption that the energy stored in a tree-like structure is dominated by the energetic stretching of strands with linear force-extension dependence. This is, however, not necessarily true since there could be many strands with higher generation indexes that are not as strongly stretched as the bridging strand and network strands with low generation indexes. Since the tension  $f_g$  in the tree decreases exponentially with the increasing generation g, very few generations will have their chains in the energetic rather than the entropic stretching regime. Below we describe how the energy is distributed in different generations of the tree structure with an emphasis on the nonlinear entropic regime.

For an illustration of our theory, we consider an example of the modified-Freely Jointed Chain (m-FJC) model,  $^{17,18}$  which is widely used in fitting the force-extension curves of polymers (**Figure 3a**). This model\_accounts for both the low-force, entropy-dominated (Langevin function  $\mathcal{L}(f/f_s)$ ) part of eq. 5), and the high-force, energy-dominated linear force-extension part (last term in eq. 5) with very large characteristic energetic tension  $f_e$ .

$$\frac{R(f)}{Nb} = \mathcal{L}\left(\frac{f}{f_s}\right) + \frac{f}{f_e} \simeq \mathcal{L}\left(\frac{f}{f_s}\right)\left(1 + \frac{f}{f_e}\right) \tag{5}$$

where R(f) is the average of end-to-end distance at force f, N is the number of Kuhn segments, b is the Kuhn Length,  $\mathcal{L}$  is the Langevin function ( $\mathcal{L}(x) = \coth(x) - x^{-1}$ ). The entropic tension  $f_s = kT/b$  characterizes the crossover between the linear Gaussian and nonlinear deformation regimes of a polymer chain, where k is the Boltzmann constant, and T is the absolute

temperature. Although in some previous studies, <sup>17</sup> the m-FJC model has also been expressed as the right-hand side of eq. 5, it is asymptotically the same as the middle part for characteristic entropic tension  $f_s$  significantly smaller than the characteristic energetic tensions  $f_s \ll f_e$ . <sup>17,18</sup> A typical value of  $f_s$  for flexible polymers with Kuhn length  $b \approx 1$  nm is  $f_s = kT/b \approx 4$  pN at room temperature. The characteristic energetic stretching tension  $f_e$  is typically three orders of magnitude higher than  $f_s$  and describes the linear energetic extension of contour length  $R/L_0 \cong 1 + f/f_e$  at  $f \ll f_e$ . Note that the polymer chain breaks at  $f_{break} \ll f_e$ .

The m-FJC model can be treated as a combined spring which consists of a conformational entropic sub-spring and an energetic stretching sub-spring connected in series (**Figure 5a, b, c**). The extensions of the conformational entropic sub-spring  $R_s$  and the energetic sub-spring  $R_e$  are additive ( $R = R_s + R_e$ ), while the tension f in both sub-springs is the same. The force-extension curve of the entropic sub-spring can be expressed by the inverse Langevin function

$$f = f_s \cdot \mathcal{L}^{-1} \left( \frac{R_s}{Nb} \right) \approx \begin{cases} 3f_s \left( \frac{R_s}{Nb} \right), \ f/f_s \ll 1 \\ \frac{f_s}{1 - R_s/(Nb)}, \ f/f_s \gg 1 \end{cases}$$
 (6)

This equation has two limits: for  $f/f_s \ll 1$  it predicts linear dependence of force on chain extension (upper approximation in eq. 6); for  $f/f_s \gg 1$  it predicts the divergence of the tension as chain extension approaches the contour length (lower approximation in eq. 6). These two limits correspond to the linear and the non-linear regimes in **Figure 5b**, respectively. <sup>19,20</sup>

The energy  $U^s(f)$  that is stored in the conformational entropic sub-spring can be obtained by integrating eq. 6 and replacing R with f, which is expressed by<sup>21,22</sup>:

$$U^{s}(f) = NkT \cdot \left[ \left( \frac{f}{f_{s}} \right) \mathcal{L} \left( \frac{f}{f_{s}} \right) + \ln \left( \frac{f/f_{s}}{\sinh(f/f_{s})} \right) \right] \approx \begin{cases} Nb \left( \frac{f^{2}}{6f_{s}} \right), \ f/f_{s} \ll 1 \\ Nb f_{s} \ln \left( f/f_{s} \right), \ f/f_{s} \gg 1 \end{cases}$$
(7)

Note this equation for the entropically-stored energy also has two limits: in the linear elasticity regime  $(f/f_s \ll 1)$ , the stored energy increases quadratically with the applied force (upper approximation in eq. 7); while in the non-linear elasticity regime  $(f/f_s \gg 1)$ , the stored energy grows logarithmically with the force (lower approximation in eq. 7). The force-extension curve of the energetic sub-spring can be described by Hooke's law  $f = f_e(R_e/Nb)$ . The energy stored per network strand in the energetic sub-spring increases quadratically with the applied tension (similar dependence as for the linear entropic regime, but with a much smaller coefficient):

$$U^{e}(f) = \frac{f^{2}}{2(f_{e}/Nb)} = NkT\left(\frac{f^{2}}{2f_{s}f_{e}}\right)$$
(8)

These energies stored in entropic and energetic sub-springs are additive ( $U = U^s + U^e$ ), thus the energy of a network strand in the m-FJC model can be written as the sum of eq. 7 and eq. 8:

$$U(f) = U^{S}(f) + U^{e}(f) = NkT \left[ \left( \frac{f}{f_{S}} \right) \mathcal{L} \left( \frac{f}{f_{S}} \right) + \ln \left( \frac{f/f_{S}}{\sinh(f/f_{S})} \right) + \frac{f^{2}}{2f_{S}f_{e}} \right]$$
(9)

The separation of the entropic component and the energetic component for each network strand allows separate analysis of the three regimes of an m-FJC, which are linear entropic, non-linear entropic, and linear energetic regimes.

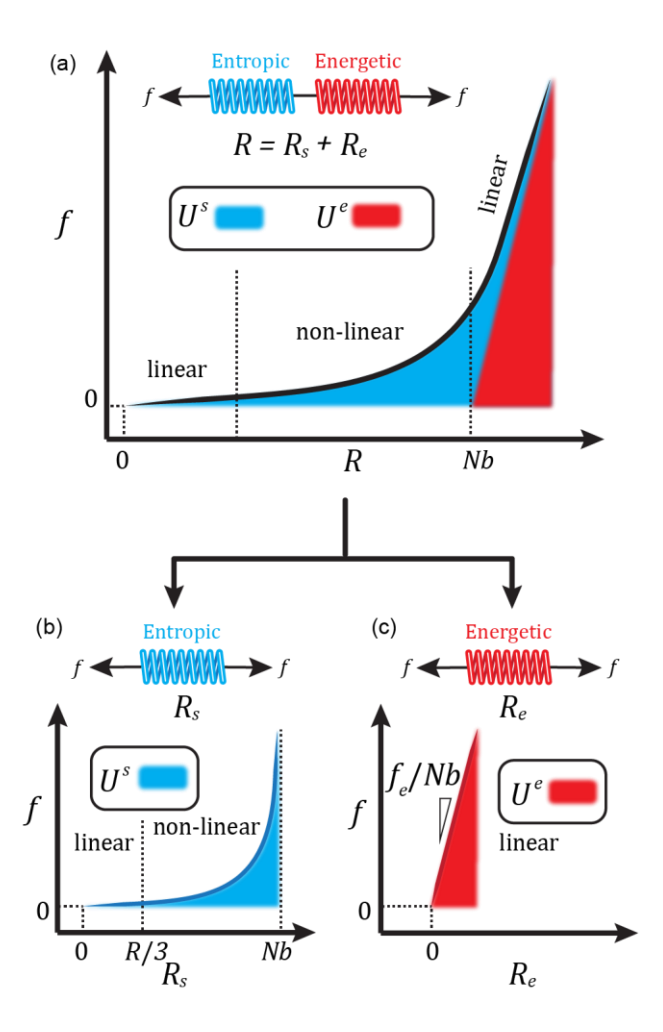


Figure 5. Schematic illustration of (a) force-extension curve f(R) for the modified Freely Jointed Chain model. (a) The m-FJC model can be treated as two sub-springs connected in series: (b) an entropic FJC sub-spring and (c) an energetic linear sub-spring. The extension of these two sub-springs is additive  $(R = R_s + R_e)$ , while the tensions are the same. The blue and red shaded areas are the energy that is stored in the entropic sub-spring  $U^s$  and the energetic sub-spring  $U^e$ , respectively. The curves are schematic, and the curvature has been exaggerated.

To illustrate the main results of our model, we first start with a specific example of a typical synthetic polymer with  $f_s \approx 7 \ pN$  and  $f_e \approx 12 \ nN$ , and  $f_e \approx 12 \ nN$ ,

breaking force of a polymer chain that has C-C or C-O as backbone bonds is  $f_{\text{break}} \approx 4.5 \, nN.^{16,24}$  For a tree with functionality z=4, which consists of strands with these parameters, the energy stored in different generations  $U_g$  can be calculated by substituting eq. 9 into eq. 3. The calculated result, shown by the black line in **Figure 6**, exhibits a nonmonotonic dependence on the absolute value of the generation index. Note that the energy per generation plotted in **Figure 6** is normalized by the energy stored in the bridging strand  $U_0$ . As |g| increases,  $U_g$  first reaches a local minimum at |g| = 2, and then reaches a local maximum at |g| = 5.

To understand this nonmonotonic variation of the energy stored in a particular generation of the tree, we separately calculate the entropic component and the energetic component by substituting eqs. 7 and 8 into eq. 3. The results for these two components are presented by blue (entropic contribution) and red (energetic contribution) lines in **Figure 6**.

Since the energetic contribution  $U^e(f_g)$  stored in network strands is described by the Hookean linear deformation (eq. 8) of network strands (**Figure 5a** and **5c**, energetic linear regime), the combined energetic component  $U_g^e$  of the energy stored in generation g exponentially decays with the generation index |g| (red line in **Figure 6**) as predicted by the Lin-Zhao model. The reason for this exponential decay is that the energy stored in a network strand  $U^e(f_g) = U^e(f_0)/(z-1)^{2|g|}$  decreases exponentially very fast with |g| and cannot be compensated by the exponential but slower increase in the number of network strands in this generation  $(z-1)^{|g|}$ . Therefore, if we only consider the energetic component, the energy stored in the bridging strand dominates the energy of the energetic component of the tree, and the total energy in the energetic component converges to  $\sum_g U_g^e(f_{break}) = \left[\frac{z}{(z-2)}\right] U^e(f_{break})$ , which is the prediction of the Lin-Zhao model. <sup>10</sup>

The entropic component of the stored energy in the bridging strand (g = 0) is indeed negligible in comparison to the energetic component,  $^{12}$  but the entropic component of the energy stored in generation g of the tree increases significantly as |g| increases and dominates the energy  $U_g$  for  $|g| \ge 2$  (blue line in **Figure 6**). The tension  $f_g$  in the first several generations, is larger than the characteristic conformational force  $(f_g \gg f_s)$  and therefore the energy of the entropic component  $U^s(f_g)$  is dominated by the non-linear elasticity, which is given by the second limit  $(f \gg f_s)$  of eq. 7:  $U^s(f) \approx Nbf_s \ln (f/f_s)$ . In this regime, the energy stored in a network strand decreases linearly with the generation index |g|:

$$U^{s}(f_{g}) = U^{s}\left(\frac{f_{0}}{(z-1)^{|g|}}\right) \approx Nb\left[f_{s}\ln\left(\frac{f_{0}}{f_{s}}\right) - |g|f_{c}\ln(z-1)\right]$$
(10)

The exponential increase in the number of network strands  $(z-1)^{|g|}$  is much stronger than this linear decrease of  $U^s(f_g)$ . This is the reason why  $U_g$  (black line in **Figure 6**) varies non-monotonically with increasing generation index |g|. After the entropic component reaches its maximum, the tension in network strands in these higher generations decreases below the characteristic entropic tension  $(f_g < f_s)$ . The entropic component  $U^s(f_g)$  in higher generation strands is dominated by the entropic linear elasticity, which is described by the first limit  $(f \ll f_s)$  of eq. 7. Since the force-extension dependence in these higher generation strands obeys Hooke's law (analog to the energetic component, but with a much smaller coefficient), the energy  $U_g^s$  decreases exponentially with the generation index |g| in this regime.

To summarize, the results in **Figure 6**, based on typical experimental data, indicate that the energy stored in the tree can be dominated by the energy stored in generations other than the bridging strand itself. The network strands in generations that dominate stored energy are in the

non-linear entropic regime (**Figure 5a**). The total energy  $U_g$  stored in these generations increases with the generation index |g| while the energy stored in generations corresponding to linear energetic and entropic regimes decreases exponentially with |g|.

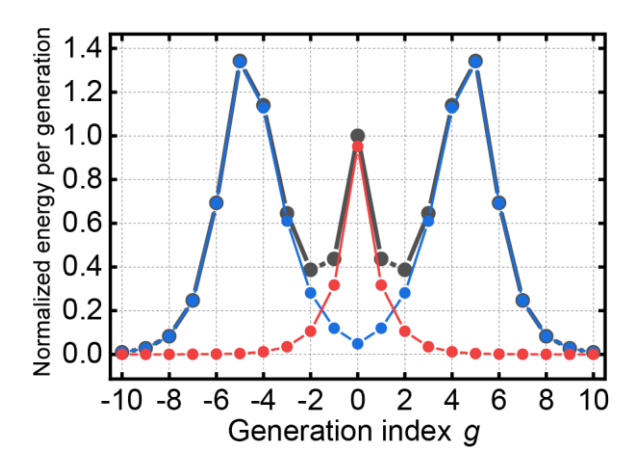


**Figure 6.** In the m-FJC model, the energy stored in generation g of a tetra-functional tree, normalized by  $U_0(f_{break})$ , is plotted in black, and its entropic and energetic components are plotted in blue and red, respectively. The parameters used in this plot are  $f_s \approx 7$  pN,  $f_e \approx 12$  nN,  $f_{break} \approx 4.5$  nN, and z=4.

Below we provide a quantitative analysis of the condition that gives  $U_g$  local maximum or minimum according to the area under the force-extension curve. Because the tree is symmetric, let us only consider the positive generations. Recall from eq. 2 and eq. 3, that the energy  $U_g$  stored in generation g can be expressed by

$$U_g = (z-1)^g \int_0^R f(R') dR' = \frac{f_0}{f(R)} \int_0^R f(R') dR'$$
 (11)

The condition that gives the local maximum or minimum of  $U_g$  is given by  $dU_g/dR = 0$  (since each generation g has a corresponding R). This condition can be rewritten as:

$$\int_0^{R_m} f(R) dR = \frac{f_m^2}{\left(\frac{df_m}{dR_m}\right)} \tag{12}$$

where  $R_m$  and  $f_m$  are the corresponding extension and force of a strand in the generations that gives the local maximum or minimum of  $U_g$ . The left-hand side of eq. 12 is the area under the force-extension curve U to the point  $(R_m, f_m)$  (blue + red areas in **Figure 7a**). To understand the meaning of the right-hand side of eq. 12, we write the equation of the tangent line at the point  $(R_m, f_m)$  (**Figure 7a** red dash line):

$$f_{\tan}(R) = f_m + \frac{df_m}{dR_m}(R - R_m)$$
(13)

The base length of the red triangle (**Figure 7a**) is given by  $(R_m - R_{tan}) = f_m/(df_m/dR_m)$ , where  $R_{tan}$  is the intercept of the tangent line on R axis. The size of the red triangle can be written as:  $\frac{1}{2}(R_m - R_{tan})f_m = \frac{1}{2}f_m^2/(df_m/dR_m)$ , which is half of the right-hand side of eq. 12. This result indicates that for the strands of generations that give the local maximum or minimum of  $U_g$ , the area of the red triangles in the force-extension curves of these strands is equal to the blue areas. For each extension and its corresponding force (R, f) on the curve, we shall define  $\gamma$  as the ratio between the area of the red triangle  $(\frac{1}{2}f^2/(df/dR))$  and the area under the force-extension curve U.

$$\gamma = \left[\frac{f^2}{2\left(\frac{df}{dR}\right)}\right]/U\tag{14}$$

When  $\gamma = 1/2$ , the blue, and the red areas are equal, and the energy  $U_g$  reaches its local maximum or minimum (**Figure 7b, c**). Essentially, the area of the red triangle of a network strand can be considered as the energy of an effective Gaussian spring which has the same

Stiffness as the strand itself at the corresponding force and extension. When this effective Gaussian spring dominates the energy stored in strands ( $\gamma > 1/2$ ), the energy  $U_g$  decreases with increasing g, which corresponds to the red and pink sections in **Figure 7b**,  $\mathbf{c}$ . These two intervals of generation g correspond to strands that are in the energetic (for small values of g) and the linear entropic (for large generations g) regimes shown in **Figure 5a**, respectively. When the blue area in Fig. 7a dominates the energy stored in strands ( $\gamma < 1/2$ ), the energy  $U_g$  increases with the generation index g, which corresponds to the non-linear entropic regime (**Figure 5a** & light blue section in **Figure 7b**,  $\mathbf{c}$ ).

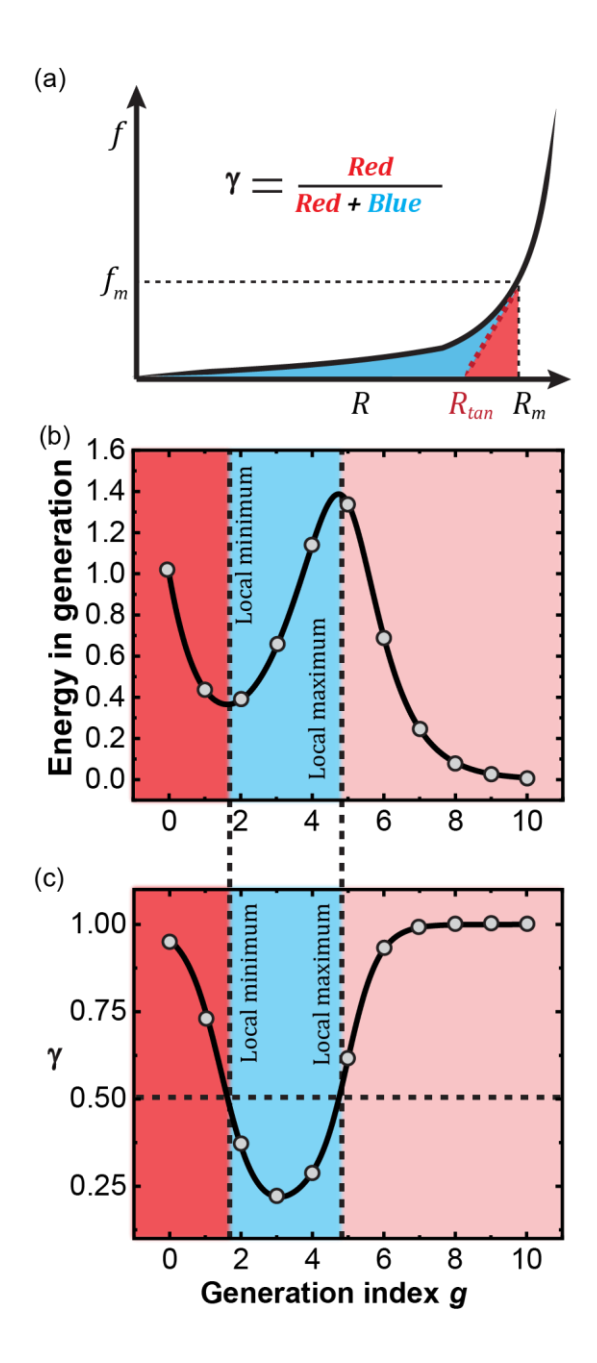


Figure 7. (a) The schematic force-extension curve of the network strand with extension  $R_m$  and force  $f_m$  of a strand in the generations that gives the local maximum or minimum of  $U_g$ .  $R_{tan}$  is the intersection of the tangent line (red dashed line) with extension R axis, and  $\gamma$  is the ratio of the area of the red triangle and the area under the force-extension curve (red + blue). The corresponding schematic plots of  $U_g$  vs. g and  $\gamma$  vs. g are presented in (b) and (c). The regimes

shaded with red and blue colors indicate the energy  $U_g$  in corresponding regimes is dominated by the red triangle and blue area in fig. (a), respectively.

For the polymer networks with finite loops, attention should be paid to the interconnection of a tree with other trees that form many loops at higher generations.<sup>8,9,14</sup> The generations that go beyond the scale of the loop cannot be simply treated as a part of one tree as they are shared by multiple trees. Since there are many loops formed above the scale of topological loop sizes, we expect the network on larger scales to be considered by continuum mechanics and the energy term  $\widehat{U}_{break}$  should be cut off by topological loop sizes.

In summary, the energy stored in the tree is determined by the functionality z, the breaking tension of the bridging strand  $f_{break}$ , the shape of the force-extension curve f(R) (e.g., for the m-FJC, it is controlled by  $f_s$  and  $f_e$ ), and the topological loop sizes. If we consider networks with different loop sizes but with the same other parameters, the energy stored in the tree with a larger number of generations in its loops is significantly larger before  $U_g$  reaches its maximum due to the contribution of the non-monotonic change in  $U_g$  (Figure 3b), although this effect becomes saturated for larger trees when strands in high generations are in the linear entropic regime. Hence, networks prepared by end-linking chains with the same degree of polymerization at higher concentrations with stronger overlap between chains are expected to be tougher, even when investigated and compared at the same final volume fraction. This effect is expected to increase weakly (logarithmically) with preparation concentration.<sup>8,9</sup> If we consider networks with different chain-breaking forces  $f_{break}$  but with the same other parameters,<sup>25</sup> then a network with a lower  $f_{break}$  would have a higher contribution from the entropic component (Figure S3a,b) and the stored energy cannot be simply estimated using the Lin-Zhao model. Similarly, if we

consider networks with different characteristic energetic tensions  $f_e$  with the same other parameters, the network with higher  $f_e$  would have a larger contribution from the entropic component (**Figure S3c**). A typical case of a network consisting of sub-chains with a high  $f_e$  is a PEG network. The PEG chain is known to have a much higher  $f_e$  (~105 nN) than conventional covalent hydrocarbon polymers ( $f_e = 20 \sim 30$  nN). For PEG networks, even the energy stored in g=1 is expected to be almost the same as that stored in the bridging strand (**Figure S3c, d**). The influence of functionality z and the characteristic entropic tension can also be found in **Figure S3e-f**.

Effect of mechanophores. In a previous study,  $^{26}$  it was shown that the addition of mechanophores (MP) with stored length toughens polymer networks through reactive strand extension. As predicted in our previous work,  $^{27}$  one might expect that the incorporation of higher force mechanophores should toughen the network more, since the reactive strand extension at high force dissipates more energy. This conclusion was made on the basis of the Lake-Thomas theory. However, the strands in the second and third generations of the tree also experience considerably large forces (on the order of  $\sim 100 \text{ pN}$ ) when the bridging strand is at its breaking tension (4  $\sim 5 \text{ nN}$ ). Although high-force mechanophores provide more energy dissipation in the bridging strand, they can only be activated in the bridging strand. Low-force mechanophores with the same stored length, however, dissipate less energy in the bridging strand due to their low activation forces, but they are more likely to be activated in other generations with many more mechanophores and could therefore dominate the dissipation of energy.

To explore this effect, we choose two characterized mechanophores as examples, which have activation forces ca. 0.7 nN and 2.1 nN at reaction rate constants ca. 2 s<sup>-1</sup>, respectively.<sup>27</sup> The

force-extension curves of network strands that consist of these two mechanophores are separately plotted in Figure 8a with the set of parameters described above ( $f_s \approx 7$  pN,  $f_e \approx 12$  nN,  $f_{\rm break} \approx 4.5$  nN, and z = 4). The total stored length released by the mechanophores is set to Nb, which doubles the contour length of the strands upon release. The increase in contour length due to the stored length release is assumed to be the same for both mechanophores. The area under the red curve is much larger than that under the blue curve, which indicates the mechanophore with a larger transition force dissipates ca. 60% more energy on the single-chain level with the set of parameters described above (this difference could range from ca. 50% ~ 200% depending on the parameters of the chain). However, when we plot the energy-force curves (Figure 8b) of tree-like structures that consist of these two types of mechanophores, there are two force transitions for the tree containing 0.7 nN mechanophores, while there is only one for the tree containing 2.1 nN mechanophores. This is because the mechanophores with 0.7 nN are not only activated in the bridging strand (g = 0), but also in generations |g| = 1, before the bridging strand breaks (Figure 8c). Since the tension is shared by 3 network strands in generation g = -1and g = 1, when mechanophores in these three strands are activated at  $\sim 700$  pN, the whole generation is bearing  $\sim 2.1$  nN tension. In other words, the mechanophores with 0.7 nN in |g| = 1 are working effectively as mechanophores with 2.1 nN in combined chains (See SI for details). Therefore, the mechanophore with 0.7 nN provides ca. 60% more energy dissipation in the tree in comparison to the mechanophore with 2.1 nN with the set of parameters described above. This effect would be more significant if we consider a trifunctional tree, in which the mechanophores with 0.7 nN activation force can be activated in generations |g| = 0, 1, 2 (Figure S4) if the bridging strand breaks at 4.5 nN.

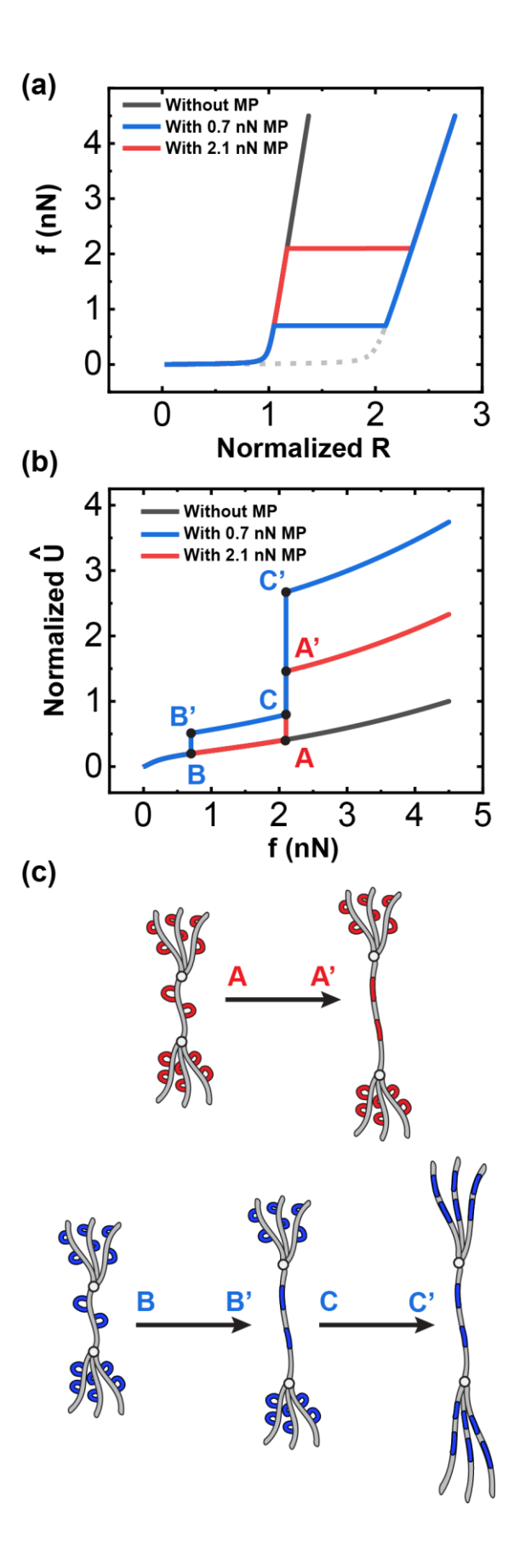


Figure 8. (a) Force-extension curves of single m-FJC network strands for typical data ( $f_s \approx 7$  pN,  $f_e \approx 12$  nN,  $f_{\rm break} \approx 4.5$  nN) that contain different mechanophores (MP) with different activation forces (blue 0.7 nN and red 2.1 nN). The transition plateaus are assumed to have constant force. The contour length of the network strand is assumed to be doubled after transition (the additional contour length of Nb is released from the stored length of mechanophores). (b) energy-force curves  $\hat{U}(f)$  of the tree (z=4) that consists of generations g from -2 to 2 made from the corresponding m-FJC network strands in fig. (a). Since the analytical form of  $\hat{U}(f)$  is complicated, we calculate them numerically. The energy  $\hat{U}$  in (b) is normalized by the energy stored in the tree without mechanophore at 4.5 nN. (c) Schematic illustration of different MPs (red 2.1 nN and blue 0.7 nN) activation in the tree-like structure before the bridging strand breaks.

As discussed above, the incorporation of mechanophores with higher activation force does not necessarily result in tougher polymer networks in this tree model. In contrast, "weaker" mechanophores have more opportunities to be activated in other unbroken strands, and they work effectively as "strong" mechanophores in generations other than the bridging strand. A more general approach considering the tree with complex chain extension is provided in the SI.

Conclusion. We modify the Lake-Thomas theory by taking into account the contribution of the energy stored in the tree-like structure to the energy parameter  $\widehat{U}_{break}$ . With the reported experimental and computational data of force-extension curve f(R) and the breaking force  $f_{break}$ , the energy stored in other unbroken network strands that are part of the tree structure is estimated to be significant in comparison to that stored in the bridging strand at the break. An unexpected non-monotonic dependence of the energy  $U_g$  stored in generation |g| on the

generation index is due to the non-linear entropic elasticity of polymer chains. We provide a geometric interpretation and show that the non-linear entropic elasticity is inherently different from the other two elasticities (linear entropic and linear energetic). We further introduce the concept of the topological loop size as the scale that determines the size of the tree-like structure. Depending on the parameters  $(z, f_{\text{break}}, f_s, f_e)$ , the loop size, etc.) of the network, the energy stored in the tree could be dominated by the energy stored in the bridging strand or energy stored in higher generations. Although we apply the m-FJC model with a linear energetic stretching in this current work, we note that there could be some nonlinear elasticity in the high force regime (> 3 nN), which has seldom been captured by the single-molecule force spectroscopy up to  $\sim 2.5$  nN.  $^{18,23,28,29}$  Since only the bridging strand is likely to experience such high force regime, we expect that this non-linearity has a minor effect on the energy stored in the tree.

Another intriguing conclusion of our model is related to the incorporation of mechanophores with stored length into networks. We suggest that lower force mechanophores could enhance the fracture energy even more than high force mechanophores in the cases when low force mechanophores can be activated both in the bridging strand and in network strands of generations |g| > 0 before the bridging strand breaks. We show that such low-force mechanophores would dissipate more energy than a high-force mechanophore that can be activated only in the bridging strand. We propose that continued advancements in strand extensional behavior, and mechanophore design, combined with techniques to control and characterize polymer network topology, can lead to better predictive models and a more insightful understanding of network fracture mechanics.

ASSOCIATED CONTENT

**Supporting Information.** 

Tree-like structure as combined chain, tree-like structure with extra inclusion, energy distribution

with different parameters, and dependence of the energy stored in a trifunctional tree with

mechanophores on the tension in the bridging strand.

**AUTHOR INFORMATION** 

**Corresponding Author** 

Email: panyukov@lpi.ru, stephen.craig@duke.edu, michael.rubinstein@duke.edu

**Author Contributions** 

The manuscript was written through contributions of all authors. All authors have given approval

to the final version of the manuscript.

**Notes** 

The authors declare no competing financial interest.

**ACKNOWLEDGMENT** 

This work was supported by the NSF Center for the Chemistry of Molecularly Optimized

Networks (MONET), CHE-2116298. We thank B. Olsen and M. Ciccotti for helpful discussions.

REFERENCES

(1) Lake, G. J.; Thomas, A. G. The Strength of Highly Elastic Materials. *Proc. R. Soc.* 

London, Ser. A Math. Phys. Sci. 1967, 300 (1460), 108–119.

(2) Rivlin, R. S.; Thomas, A. G. Rupture of Rubber. I. Characteristic Energy for Tearing. J.

28

- Polym. Sci. 1953, 10 (3), 291–318.
- (3) Zehnder, A. T. Fracture Mechanics; Springer London Dordrecht Heidelberg New York, 2012.
- (4) Lake, G. J.; Lindley, P. B. The Mechanical Fatigue Limit for Rubber. J. Appl. Polym. Sci. 1965, 9, 1233–1251.
- (5) Akagi, Y.; Sakurai, H.; Gong, J. P.; Chung, U. I.; Sakai, T. Fracture Energy of Polymer Gels with Controlled Network Structures. *J. Chem. Phys.* **2013**, *139* (14), 144905.
- Barney, C. W.; Ye, Z.; Sacligil, I.; McLeod, K. R.; Zhang, H.; Tew, G. N.; Riggleman, R.
  A.; Crosby, A. J. Fracture of Model End-Linked Networks. *Proc. Natl. Acad. Sci. U. S. A.*2022, 119 (7).
- (7) Slootman, J.; Waltz, V.; Yeh, C. J.; Baumann, C.; Göstl, R.; Comtet, J.; Creton, C. Quantifying Rate- and Temperature-Dependent Molecular Damage in Elastomer Fracture. *Phys. Rev. X* **2020**, *10* (4), 041045.
- (8) Cai, L. H.; Panyukov, S.; Rubinstein, M. Hopping Diffusion of Nanoparticles in Polymer Matrices. *Macromolecules* **2015**, *48* (3), 847–862.
- (9) Panyukov, S. Loops in Polymer Networks. *Macromolecules* **2019**, *52*, 4145–4153.
- (10) Lin, S.; Zhao, X. Fracture of Polymer Networks with Diverse Topological Defects. *Phys. Rev. E* **2020**, *102*, 52503.
- (11) Williams, J. G. Fracture Mechanics of Polymers; Ellis Horwood: Chichester, 1984.
- (12) Wang, S.; Panyukov, S.; Rubinstein, M.; Craig, S. L. Quantitative Adjustment to the Molecular Energy Parameter in the Lake–Thomas Theory of Polymer Fracture Energy.

- Macromolecules 2019, 52, 2772–2777.
- (13) Wang, S.; K. Beech, H.; H. Bowser, B.; B. Kouznetsova, T.; D. Olsen, B.; Rubinstein, M.; L. Craig, S. Mechanism Dictates Mechanics: A Molecular Substituent Effect in the Macroscopic Fracture of a Covalent Polymer Network. J. Am. Chem. Soc. 2021, 143 (10), 3714–3718.
- Michalke, W.; Lang, M.; Kreitmeier, S.; Göritz, D. Comparison of Topological Properties between End-Linked and Statistically Cross-Linked Polymer Networks. *J. Chem. Phys.* 2002, 117 (13), 6300.
- (15) Grandbois, M.; Beyer, M.; Rief, M.; Clausen-Schaumann, H.; Gaub, H. E. How Strong Is a Covalent Bond. *Science* **1999**, *283* (5408), 1727–1730.
- (16) Beyer, M. K. The Mechanical Strength of a Covalent Bond Calculated by Density Functional Theory. *J. Chem. Phys.* **2000**, *112* (17), 7307–7312.
- (17) Smith, S. B.; Cui, Y.; Bustamante, C. Overstretching B-DNA: The Elastic Response of Individual Double-Stranded and Single-Stranded DNA Molecules. *Science* **1996**, *271* (9), 795–799.
- (18) Oesterhelt, F.; Rief, M.; Gaub, H. E. Single Molecule Force Spectroscopy by AFM Indicates Helical Structure of Poly(Ethylene Glycol) in Water. *New J. Phys.* **1999**, *1*, 6.
- (19) Kuhn, W. Über Die Gestalt Fadenförmiger Moleküle in Lösungen. *Kolloid-Zeitschrift* 1934 681 **1934**, 68 (1), 2–15.
- (20) Flory, P. J. *Principles of Polymer Chemistry*; Cornell University Press: Ithaca, NY, and London, 1953.
- (21) Mao, Y.; Talamini, B.; Anand, L. Rupture of Polymers by Chain Scission. Extrem. Mech.

- *Lett.* **2017**, *13*, 17–24.
- (22) Arora, A.; Lin, T.-S.; Beech, H. K.; Mochigase, H.; Wang, R.; Olsen, B. D. Fracture of Polymer Networks Containing Topological Defects. *Macromolecules* **2020**, *53*, 7346–7355.
- (23) Zhang, W.; Zhang, X. Single Molecule Mechanochemistry of Macromolecules. *Prog. Polym. Sci.* **2003**, *28* (8), 1271–1295.
- (24) Lebedeva, N. V; Nese, A.; Sun, F. C.; Matyjaszewski, K.; Sheiko, S. S. Anti-Arrhenius Cleavage of Covalent Bonds in Bottlebrush Macromolecules on Substrate. *Proc. Natl. Acad. Sci. U. S. A.* **2012**, *109*, 9276–9280.
- (25) Wang, S.; Beech, H. K.; Bowser, B. H.; Kouznetsova, T. B.; Olsen, B. D.; Rubinstein, M.; Craig, S. L. Mechanism Dictates Mechanics: A Molecular Substituent Effect in the Macroscopic Fracture of a Covalent Polymer Network. *J. Am. Chem. Soc.* 2021, 143 (10), 3714–3718.
- (26) Wang, Z.; Zheng, X.; Ouchi, T.; Kouznetsova, T. B.; Beech, H. K.; Av-Ron, S.; Matsuda, T.; Bowser, B. H.; Wang, S.; Johnson, J. A.; Kalow, J. A.; Olsen, B. D.; Gong, J. P.; Rubinstein, M.; Craig, S. L. Toughening Hydrogels through Force-Triggered Chemical Reactions That Lengthen Polymer Strands. *Science* 2021, 374 (6564), 193.
- (27) Bowser, B. H.; Wang, S.; Kouznetsova, T. B.; Beech, H. K.; Olsen, B. D.; Rubinstein, M.; Craig, S. L. Single-Event Spectroscopy and Unravelling Kinetics of Covalent Domains Based on Cyclobutane Mechanophores. *J. Am. Chem. Soc* **2021**, *143* (13), 5269–5276.
- (28) Wang, J.; Kouznetsova, T. B.; Boulatov, R.; Craig, S. L. Mechanical Gating of a Mechanochemical Reaction Cascade. *Nat. Commun.* **2016**, *7*, 13433.

(29) Sammon, M. S.; Schirra, S.; Pill, M. F.; Clausen-Schaumann, H.; Beyer, M. K. Functionalization of Diamond-Like Carbon Surfaces to Access High Rupture Forces in Single-Molecule Force Spectroscopy of Covalent Bonds. *Chem. - Methods* **2021**, *1* (6), 271–277.

## For Table of Contents use only

